Magnetic circular dichroism anisotropy from coherent Raman detected electron paramagnetic resonance spectroscopy: Application to spin-1/2 transition metal ion centers in proteins

Stephen J. Bingham
Department of Physics, University of Bath, Bath, BA2 7AY, England

Jörg Gutschank, Birgit Börger, and Dieter Suter
Fachbereich Physik, Universität Dortmund, D-44221 Dortmund, Germany

Andrew J. Thomson
Centre for Metalloprotein Spectroscopy and Biology, School of Chemical Sciences,
University of East Anglia, Norwich, NR4 7TJ, England

Measurement of magnetic circular dichroism (MCD) anisotropy has contributed greatly to the understanding of the electronic structure of transition metal ion centers in both biological and nonbiological materials. Compared to previous methods, optically detected electron paramagnetic resonance experiments can measure MCD anisotropy with dramatically improved orientational resolution. In this paper the relevant theory for systems with an isolated Kramers doublet ground level is derived and its application illustrated using a transition metal ion center in a protein: low spin ferric haem. © *2000 American Institute of Physics.* [S0021-9606(00)00634-6]

I. INTRODUCTION

Magnetic circular dichroism (MCD) anisotropy is a powerful tool in the assignment of electronic transitions and hence in the understanding of molecular structure.[1,2] The MCD field and temperature dependencies of samples containing randomly oriented molecules are sensitive to this anisotropy.[3–6] Such experiments, which are known as MCD magnetization or saturation curve analysis, have been particularly important in the study of transition metal ion centers in enzymes and other proteins. When combined with information from complementary methods, such as optical absorption and electron paramagnetic resonance spectroscopies, it has been possible to deduce the chemical structures of paramagnetic centers.[2] However, MCD magnetization experiments rely on the ability to distinguish between centers with different orientations through their different Boltzmann spin polarizations. As the magnetic anisotropy of the centers decreases, the requirements for instrumental linearity, stability, and signal-to-noise can become very severe.[6]

Electron paramagnetic resonance (EPR) methods[7,8] are able to distinguish between centers with different orientations relatively easily using the microwave resonance condition. In an ideal optically detected EPR experiment one therefore performs an optical experiment on an orientationally selected set of chromophores. If MCD is used to detect the EPR we may therefore, in principle, measure the MCD anisotropy with high accuracy. The first attempts to exploit this possibility in samples containing randomly oriented molecules[9,10] used a relatively well-known method[11,12]—saturation of the EPR transition by the resonant microwave radiation and detection of the subsequent reduction in the MCD signal. Unfortunately, although successful experiments were carried out on several types of copper protein,[9,10] a number of severe difficulties were experienced. Experimentally, it is difficult to distinguish between anisotropy of the microwave saturation/magnetic relaxation and MCD anisotropy. In addition, magnetic relaxation effects (cross-relaxation[13] and spectral diffusion) can remove the orientational selectivity of the experiment: Molecules which are not resonant with the microwaves become saturated. These magnetic relaxation/microwave saturation effects are also strongly dependent upon sample variables such as concentration and other experimental conditions. Understanding these effects can be especially difficult in proteins containing multiple paramagnetic centers.

The coherent Raman detected EPR experiment has the potential to overcome these difficulties. Like the conventional microwave detected EPR experiment,[7,8] coherent Raman detected EPR measures the microwave induced precession of the sample magnetization. The fundamental nature of the coherent Raman process[14–16] means that there are potentially many different types of experiment belonging to this class. An important group of coherent Raman detected EPR experiments, which are the principal subject of this paper, are those that may be considered to arise from an oscillating magnetic circular dichroism or birefringence (Faraday rotation) due to the microwave-induced precessing magnetization.[17–20] We find it convenient to refer to experiments of this class as ''PROD'' experiments (Paramagnetic Resonance Optically Detected). It is possible to measure MCD anisotropy using the PROD experiment.[21] Other types of coherent Raman detected EPR experiments have been performed that cannot be described in terms of an oscillating MCD or Faraday rotation.[22]

The difficulties experienced with conventional MCD detected EPR arise from the fact that strictly speaking it does

4331

not measure EPR at all but rather a secondary consequence: repopulation of the magnetic states by microwave power saturation. In contrast, the PROD experiment measures EPR in as direct a way as can be envisaged with an optical experiment. This fundamental simplicity makes the experiment more suitable for precision measurements of MCD anisotropy. In the absence of microwave saturation, the only potential influence of magnetic relaxation effects on the size of the precessing magnetization is through the EPR line shape function. In many practical cases other factors determine the line shape,[7,8] and in the rare cases where relaxation is important it is usually not necessary to know the details of the mechanism in order to simulate the spectra. Equally importantly, the interactions between paramagnetic centers that, through cross-relaxation, can remove orientational selectivity in MCD detected EPR at worse only influence line shape in coherent Raman detected EPR. If it is possible to distinguish between centers by conventional microwave detected EPR then it will also be possible to do so with coherent Raman detected EPR. These considerations lead to a dramatic simplification of the interpretation of the experiment.

Recent instrumental improvements[23] allow the PROD experiment to be applied to a remarkably wide range of scientific problems. It is the purpose of this paper to illustrate how MCD anisotropy can be measured using the PROD experiment. To this end, a theoretical treatment of molecules with fictitious spin-1/2 ground levels is given and the theory is compared to an experiment on a metalloprotein: low spin ferric haem (*Pseudomonas aeruginosa* cytochrome c551). We refer to ''fictitious'' spin to remind ourselves that the states concerned are never pure spin functions.

II. THEORY

A. Basic equations

We consider a molecule (or, more generally, a localized chromophore such as an ion, atom, or defect center) with a fictitious spin-1/2 ground level. We assume that other levels have no significant thermal population and are not mixed into the ground level by the applied magnetic field. In short, we are concerned with a molecule whose ground level may be described with a $\tilde{S}=1/2$ spin Hamiltonian. We further assume that the dominant contribution to the MCD arises from the thermal spin polarization of the ground level. This is nearly always the case for transition metal ion paramagnets at cryogenic temperatures. For such a molecule the MCD along a laboratory axis P may be related to the molecular fictitious spin expectation values, $\langle \tilde{S}_{xyz} \rangle$, through the equation:

$$\Delta\varepsilon_P = 4Kf(\nu,\Delta)[(A_{Px}C_{xx}+A_{Py}C_{yx}+A_{Pz}C_{zx})\langle\tilde{S}_x\rangle$$
$$+(A_{Px}C_{xy}+A_{Py}C_{yy}+A_{Pz}C_{zy})\langle\tilde{S}_y\rangle$$
$$+(A_{Px}C_{xz}+A_{Py}C_{yz}+A_{Pz}C_{zz})\langle\tilde{S}_z\rangle], \quad (1)$$

where $\Delta\varepsilon_P$ is the difference between molar extinction coefficients for left and right circularly polarized light (ε_L
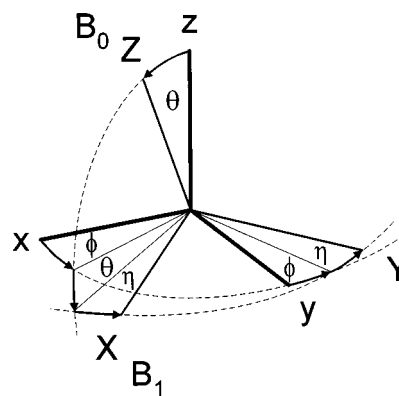

FIG. 1. Euler angles ϕ, θ, η relating the molecular g-value axis system x, y, z and the laboratory axis system X, Y, Z. The main magnetic field B_0 is applied along Z and the linearly polarized microwave frequency field $2B_1 \cos \omega t$ is applied along X. In practical instruments B_0 will normally be horizontal. The directional cosines used throughout the main text are: $A_X = (\cos\theta\cos\phi\cos\eta - \sin\phi\sin\eta, \cos\theta\sin\phi\cos\eta + \cos\phi\sin\eta, -\sin\theta\cos\eta)$, $A_Y = (-\cos\theta\cos\phi\sin\eta - \sin\phi\cos\eta, -\cos\theta\sin\phi\sin\eta + \cos\phi\cos\eta, \sin\theta\sin\eta)$, and $A_Z = (\sin\theta\cos\phi, \sin\theta\sin\phi, \cos\theta)$.

$-\varepsilon_R$), K is a collection of fundamental constants $(N_A\alpha^2\pi\log(e)/1000\hbar\varepsilon_0 c\,\eta)$, $f(\nu,\Delta)$ is a magnetic field independent optical line shape function with a normalized zeroth moment

$$\left(\int \frac{f(\nu,\Delta)}{\nu}d\nu = 1\right),$$

and the A_{Pi} are the directional cosines between the optical propagation axis P and the ith molecular axis, $i=xyz$. The parameters C contain the optical matrix elements:

$$C_{xi} = \sum_e \text{Im}\{\langle g(i)|m_y|e\rangle\langle e|m_z|g(i)\rangle\},$$

$$C_{yi} = \sum_e \text{Im}\{\langle g(i)|m_z|e\rangle\langle e|m_x|g(i)\rangle\},$$

$$C_{zi} = \sum_e \text{Im}\{\langle g(i)|m_x|e\rangle\langle e|m_y|g(i)\rangle\},$$

where the m_i are the linearly polarized electric transition dipole operators in the molecular frame, $|e\rangle$ are the excited level states, and $|g(i)\rangle$ are the ground level states with their fictitious spins quantized along each molecular axis, i. These expressions are derived in Appendix A.

B. MCD magnetization/saturation curve analysis

The most important method of studying MCD anisotropy used at present is the magnetization/saturation experiment.[1,3–6] In this technique the circular dichroism experienced by an optical beam propagating parallel to an applied magnetic field, B_0, is studied as a function of magnetic field strength and temperature. In order to firmly establish the connection with our PROD experiments we shall derive the relevant theory for this experiment. Considerable simpli-

fication is obtained if we equate the molecular axis system, xyz, with that of the g-value system. We consider a molecule whose g-value axes are oriented relative to the applied field axis Z in accordance with Fig. 1. We shall have numerous occasion to refer to the directional cosine A_{ji} between the ith g-value axis ($i = x, y, z$) and another axis j. The orientational dependencies of the ith component of the fictitious spin is

$$\langle \widetilde{S}_i \rangle = \langle \widetilde{S}_0 \rangle \left(\frac{g_i}{g} \right) A_{Zi},\qquad(2)$$

where $\langle \widetilde{S}_0 \rangle$ is the thermally averaged fictitious spin of the molecule: $\langle \widetilde{S}_0 \rangle = -\frac{1}{2}\tanh(g\beta B_0 / 2kT)$, g_i is the principal g-value, and $g^2 = \Sigma_i g_i^2 A_{Zi}^2$. A geometrical derivation of these equations is found in Appendix B. Combining these expressions in Eq. (1) ($P = Z$) and expressing the A_{Zi} in terms of the polar angles, Fig. 1, we obtain our explicit expression for the MCD anisotropy:

$$\Delta \varepsilon_Z = 4Kf(\nu, \Delta) \frac{\langle \widetilde{S}_0 \rangle}{g} [(C_{xx} \sin\theta\cos\phi + C_{yx}\sin\theta\sin\phi$$
$$+ C_{zx}\cos\theta)g_x \sin\theta\cos\phi$$
$$+ (C_{xy}\sin\theta\cos\phi + C_{yy}\sin\theta\sin\phi + C_{zy}\cos\theta)g_y$$
$$\times \sin\theta\sin\phi + (C_{xz}\sin\theta\cos\phi + C_{yz}\sin\theta\sin\phi$$
$$+ C_{zz}\cos\theta)g_z\cos\theta].\qquad(3)$$

In many practical applications of MCD a sample containing randomly oriented molecules is studied. Only three terms in Eq. (3) are even functions of θ and ϕ, and it is only these terms that need to be considered when simulating a magnetization curve:

$$\langle \Delta\varepsilon \rangle_Z = \frac{8}{\pi}Kf(\nu,\Delta)\int_0^{\pi/2}\int_0^{\pi/2}\frac{\langle\widetilde{S}_0\rangle}{g}[C_{xx}g_x\sin^2\theta\cos^2\phi$$
$$+ C_{yy}g_y\sin^2\theta\sin^2\phi$$
$$+ C_{zz}g_z\cos^2\theta]\sin\theta\, d\theta\, d\phi.\qquad(4)$$

For a molecule with an axially symmetric g-value system ($g_x = g_y = g_\perp$) this reduces to

$$\langle\Delta\varepsilon\rangle_Z = 4Kf(\nu,\Delta)\int_0^{\pi/2}\frac{\langle\widetilde{S}_0\rangle}{g}$$
$$\times [C_\perp g_\perp \sin^2\theta + C_{zz}g_z\cos^2\theta]\sin\theta\, d\theta,\qquad(5)$$

where $C_\perp = (C_{xx} + C_{yy})/2$.

Expressions of these mathematical forms [Eqs. (4) and (5)] have been obtained by several authors.[3,4,6] However, unlike earlier derivations, the present treatment does not rely on the presence of molecular symmetry[3,4] or the appropriateness of a particular model of electronic structure.[6]

C. PROD experiment

Excitation of a paramagnetic sample by a resonant microwave field results in precession of the magnetization about the applied magnetic field axis at the microwave frequency.[7] In the conventional EPR experiment the precessing magnetization is detected through the microwave radiation that it emits.[24] In the PROD experiment the precessing magnetization is detected through the oscillating circular dichroism (or birefringence) experienced by an optical beam propagating perpendicularly to the applied field.[17–20] We have already derived an expression for the MCD in terms of the fictitious spin expectation values, Eq. (1). The derivation of that equation does not rely on the fictitious spin expectation values being the thermal values. A light beam passing through the sample is unable to deduce the method by which the spin polarization was created. We may therefore use Eq. (1) to calculate the microwave-induced oscillating MCD subject to one important condition, i.e., that the optical linewidth is much larger than the microwave frequency. This is necessary so that the optically induced molecular electric dipole can adjust adiabatically to the precessing magnetization, or alternatively so that we may continue to use the concept of an optical transition probability on a time scale short compared to the microwave period.[18] In this circumstance we may separately treat the interaction of the optical and magnetic transitions with the radiation. It is very rare for optical transitions of paramagnetic species in condensed matter to have optical linewidths narrower than microwave (1–300 GHz, 0.03–10 cm^{-1}) frequencies. In the cases where it does occur, it is possible to perform the calculation with other methods,[14,16] but the signal is no longer solely determined by the aspects of electronic structure that give rise to MCD. These more general cases lie beyond the scope of this paper.

Calculation of the oscillating MCD therefore comes down, within the assumptions discussed above, to solving the equation of motion of the fictitious spin. We again consider a fictitious spin-1/2 molecule with a rhombic g-value system. We must specify the orientation of the microwave field relative to the g-value axes, Fig. 1. We introduce a laboratory axis system, XYZ, with the applied field, B_0, along Z and the microwave field $2B_1\cos\omega t$ applied along X. It is convenient to consider separately the parts of the fictitious spin that oscillate in phase with and in phase quadrature with the magnetization responsible for the conventional EPR signal. The oscillating fictitious spin polarizations along the g-value axes are shown in Appendix C to be

$$\langle\widetilde{S}_x\rangle_{\text{EPR}} = \left(\left(\frac{g_x g_z^2}{g^2} \right)\cos\theta\cos\phi\cos\eta \right.$$
$$+ \left(\frac{g_x(g_y^2 - g_x^2)g_z^2}{g_\perp^2 g^2} \right)\cos^2\theta\cos^2\phi\sin\phi\sin\eta$$
$$\left. - \left(\frac{g_x g_y^2}{g_\perp^2} \right)\sin\phi\sin\eta \right)$$
$$\times \frac{\langle\widetilde{S}_{\text{disp.}}\rangle\cos(\omega t) - \langle\widetilde{S}_{\text{abs.}}\rangle\sin(\omega t)}{g_1},\qquad(6)$$

$$\langle \widetilde{S}_y \rangle_{\text{EPR}} = \left(\left(\frac{g_x^2 g_y}{g_\perp^2} \right) \cos \phi \sin \eta + \left(\frac{g_y g_z^2}{g^2} \right) \cos \theta \sin \phi \cos \eta \right.$$
$$+ \left. \left(\frac{g_y(g_y^2 - g_x^2)g_z^2}{g_\perp^2 g^2} \right) \cos^2 \theta \sin^2 \phi \cos \phi \sin \eta \right)$$
$$\times \frac{\langle \widetilde{S}_{\text{disp.}} \rangle \cos(\omega t) - \langle \widetilde{S}_{\text{abs.}} \rangle \sin(\omega t)}{g_1}, \quad (7)$$

$$\langle \widetilde{S}_z \rangle_{\text{EPR}} = - \left(\left(\frac{g_\perp^2 g_z}{g^2} \right) \sin \theta \cos \eta \right.$$
$$+ \left. \left(\frac{(g_y^2 - g_x^2)g_z}{g^2} \right) \cos \theta \sin \theta \cos \phi \sin \phi \sin \eta \right)$$
$$\times \frac{\langle \widetilde{S}_{\text{disp.}} \rangle \cos(\omega t) - \langle \widetilde{S}_{\text{abs.}} \rangle \sin(\omega t)}{g_1}, \quad (8)$$

$$\langle \widetilde{S}_x \rangle_{\text{Quad.}} = - \left(\left(\frac{g_y g_z}{g} \right) \sin \phi \cos \eta \right.$$
$$+ \left(\frac{g_y(g_y^2 - g_x^2)g_z}{g_\perp^2 g} \right) \cos \theta \sin^2 \phi \cos \phi \sin \eta$$
$$+ \left. \left(\frac{g_x^2 g_y g_z}{g_\perp^2 g} \right) \cos \theta \cos \phi \sin \eta \right)$$
$$\times \frac{\langle \widetilde{S}_{\text{disp.}} \rangle \sin(\omega t) + \langle \widetilde{S}_{\text{abs.}} \rangle \cos(\omega t)}{g_1}, \quad (9)$$

$$\langle \widetilde{S}_y \rangle_{\text{Quad.}} = \left(\left(\frac{g_x g_z}{g} \right) \cos \phi \cos \eta \right.$$
$$+ \left(\frac{g_x(g_y^2 - g_x^2)g_z}{g_\perp^2 g} \right) \cos \theta \cos^2 \phi \sin \phi \sin \eta$$
$$- \left. \left(\frac{g_x g_y^2 g_z}{g_\perp^2 g} \right) \sin \phi \cos \theta \sin \eta \right)$$
$$\times \frac{\langle \widetilde{S}_{\text{disp.}} \rangle \sin(\omega t) + \langle \widetilde{S}_{\text{abs.}} \rangle \cos(\omega t)}{g_1}, \quad (10)$$

$$\langle \widetilde{S}_z \rangle_{\text{Quad.}} = \left(\frac{g_x g_y}{g} \right) \sin \theta \sin \eta$$
$$\times \frac{\langle \widetilde{S}_{\text{disp.}} \rangle \sin(\omega t) + \langle \widetilde{S}_{\text{abs.}} \rangle \cos(\omega t)}{g_1}, \quad (11)$$

where

$$g_1^2 = \left(\left(\frac{g_\perp g_z}{g} \right) \cos \eta + \left(\frac{(g_y^2 - g_x^2)g_z}{g_\perp g} \right) \right.$$
$$\left. \times \cos \phi \sin \phi \cos \theta \sin \eta \right)^2 + \left(\frac{g_x g_y}{g_\perp} \right)^2 \sin^2 \eta, \quad (12)$$

and $g_\perp^2 = g_y^2 \sin^2 \phi + g_x^2 \cos^2 \phi$.

For a microwave field sufficiently weak to avoid saturation, the absorption and dispersion phase fictitious spin polarizations are given by

$$\langle \widetilde{S}_{\text{abs.}} \rangle = -g_1 \beta B_1 \langle \widetilde{S}_0 \rangle \pi f(\omega), \quad (13)$$

$$\langle \widetilde{S}_{\text{disp.}} \rangle = -g_1 \beta B_1 \langle \widetilde{S}_0 \rangle \pi g(\omega), \quad (14)$$

where β is the Bohr magneton, $f(\omega)$ is a line shape function normalized according to $\int_0^\infty f(\omega) d\omega = 1$, and $g(\omega)$ is its Kramers–Kronig transform.[25]

We shall consider first a light beam propagating along the laboratory X axis, parallel to the microwave field B_X. Substituting the expressions for the oscillating spin polarizations and the directional cosines, Fig. 1, in Eq. (1) ($P=X$), we obtain an expression for the PROD anisotropy of a single molecule. However, the case of common practical interest is a sample containing randomly oriented molecules. Very considerable simplification is possible in this case because most terms average to zero when integrated over the angles θ, ϕ, η. Noting that g, $g_\perp$, and g_1 are even functions of θ, ϕ, η, one finds that only the three diagonal terms survive. Further, only the part of the fictitious spin oscillating in phase with the magnetization responsible for the conventional EPR signal, $\langle \widetilde{S}_i \rangle_{\text{EPR}}$, contributes to the oscillating MCD in this geometry. As long as the $f(\omega)$ is independent of η, which is normally the case, we may average over η:

$$\langle \Delta \varepsilon \rangle_X = \frac{4}{\pi} K f(\nu, \Delta) \int_0^{\pi/2} \int_0^{\pi/2} \left[C_{xx} \left(\left(\frac{g_x^3 g_z^2}{g_\perp^2 g^2} \right) \cos^2 \theta \cos^2 \phi + \left(\frac{g_x g_y^2}{g_\perp^2} \right) \sin^2 \phi \right) \right.$$
$$+ C_{yy} \left(\left(\frac{g_y^3 g_z^2}{g_\perp^2 g^2} \right) \cos^2 \theta \sin^2 \phi + \left(\frac{g_x^2 g_y}{g_\perp^2} \right) \cos^2 \phi \right) + \left. C_{zz} \left(\frac{g_\perp^2 g_z}{g^2} \right) \sin^2 \theta \right] \frac{\langle \widetilde{S}_{\text{disp.}} \rangle \cos(\omega t) - \langle \widetilde{S}_{\text{abs.}} \rangle \sin(\omega t)}{g_1} \sin \theta \, d\theta \, d\phi. \quad (15)$$

This equation is analogous to Eq. (4) in the MCD magnetization experiment, and like that equation it may be numerically integrated by computer to simulate the experiment. For a molecule with an axial g-value system, Eq. (15) reduces to

$$\langle \Delta \varepsilon \rangle_X = 2 K f(\nu, \Delta) \int_0^{\pi/2} \left[C_\perp \left(\left(\frac{g_\perp g_z^2}{g^2} \right) \cos^2 \theta + g_\perp \right) + C_{zz} \left(\frac{g_\perp^2 g_z}{g^2} \right) \sin^2 \theta \right] \frac{\langle \widetilde{S}_{\text{disp.}} \rangle \cos(\omega t) - \langle \widetilde{S}_{\text{abs.}} \rangle \sin(\omega t)}{g_1} \sin \theta \, d\theta. \quad (16)$$

An equation of this form was used by us in a previous publication.[21] In the case of an isotropic g-value system, integration over a sphere gives: $\langle \Delta \varepsilon \rangle_x = 4 K f(\nu, \Delta) C (\langle \widetilde{S}_{\text{disp.}} \rangle \cos(\omega t) - \langle \widetilde{S}_{\text{abs.}} \rangle \sin(\omega t))$, where $C = (C_{xx} + C_{yy} + C_{zz})/3$. This "atomic" case has also been considered by Dehmelt.[17]

Another possible geometry is an optical light beam propagating along Y, perpendicular to the microwave and applied fields, Fig. 1. For such a geometry one obtains (averaging over η):

$$\langle\Delta\varepsilon\rangle_Y=\frac{4}{\pi}Kf(\nu,\Delta)\int_0^{\pi/2}\int_0^{\pi/2}\Bigg[C_{xx}\Bigg(\Bigg(\frac{g_x^2g_yg_z}{g_\perp^2g}\Bigg)\cos^2\phi+\Bigg(\frac{g_y^3g_z}{g_\perp^2g}\Bigg)\sin^2\phi\Bigg)(\sin^2\phi+\cos^2\theta\cos^2\phi)$$

$$+C_{yy}\Bigg(\Bigg(\frac{g_x^3g_z}{g_\perp^2g}\Bigg)(\cos^2\phi+\cos^2\theta\sin^2\phi)\cos^2\phi+\Bigg(\frac{g_xg_y^2g_z}{g_\perp^2g}\Bigg)(\cos^2\phi\sin^2\theta+\cos^2\theta)\sin^2\phi\Bigg)+C_{zz}\Bigg(\frac{g_xg_y}{g}\Bigg)\sin^2\theta\Bigg]$$

$$\times\frac{\langle\widetilde{S}_{\text{disp.}}\rangle\sin(\omega t)+\langle\widetilde{S}_{\text{abs.}}\rangle\cos(\omega t)}{g_1}\sin\theta\,d\theta\,d\phi, \tag{17}$$

which reduces in the axial case to

$$\langle\Delta\varepsilon\rangle_Y=2Kf(\nu,\Delta)$$

$$\times\int_0^{\pi/2}\Bigg[C_\perp\Bigg(\frac{g_\perp g_z}{g}\Bigg)(1+\cos^2\theta)+C_{zz}\Bigg(\frac{g_\perp^2}{g}\Bigg)\sin^2\theta\Bigg]$$

$$\times\frac{\langle\widetilde{S}_{\text{disp.}}\rangle\sin(\omega t)+\langle\widetilde{S}_{\text{abs.}}\rangle\cos(\omega t)}{g_1}\sin\theta\,d\theta.$$

Thus in addition to a $\pi/2$ phase shift in the temporal dependence, the orientational dependence of the terms proportional to C_{xx}, C_{yy}, C_{zz}, etc. are different compared to the first geometry. The resulting PROD line shapes will also therefore be different, although the information content is the same. No net modulated circular dichroism is obtained for a light beam propagating parallel to the applied field B_0. Clearly, the case of an arbitrarily orientated light beam can be treated by considering the components of the light beam passing along X and Y, and taking an appropriate linear combination of Eqs. (15) and (17).

III. APPLICATIONS

We shall illustrate the application of the theory using a low spin ferric haem protein: *Pseudomonas aeruginosa* cytochrome c_{551}. Low spin ferric haems perform electron transfer functions in a variety of biochemical processes.[26] The buffered protein solution was mixed with a glassing agent (glycerol 1:1 by volume) to obtain an optically transparent sample when frozen. The centers are therefore randomly orientated. All data were measured with a microwave frequency optical heterodyne detected instrument described in detail elsewhere.[19,21,23] The intensity modulation of the transmitted light beam was measured using a high speed photodiode and low noise microwave receiver. A single microwave oscillator is used to excite the sample and drive the microwave receiver. This allows the phase relationship between the microwave excitation and the optical modulation to be examined and hence the signals due to the absorptive, $\langle\widetilde{S}_{\text{abs.}}\rangle$, and dispersive, $\langle\widetilde{S}_{\text{disp.}}\rangle$, parts of the precessing fictitious spin to be measured separately. The data are presented in terms of the microwave modulation of the absorbance ΔA of circularly polarized light according to: $P=P_0\cdot10^{-A}$, $A=A_0+(\Delta A/2)\sin(\omega t)$, where P is the transmitted optical power, P_0 is the incident power, $\omega/2\pi$ is the microwave frequency, and A_0 is the average absorbance. Unlike conven-

tional EPR instruments, no magnetic field modulation is used so spectra and simulations are presented as the absolute signal rather than its first derivative. Spectra have the same sign as the conventional EPR spectra when the MCD giving rise to them is positive.

Simulations are carried out using numerical orientational averaging methods closely analogous to those used in conventional EPR.[8] The major differences arise from the need to simulate the dispersion phase signal. For this reason a complete frequency-space spectrum is simulated for each magnetic field point. A considerable (typically two order of magnitude) increase in computation time results from this approach relative to field-space calculations. It is also important to note that the Kramers–Kronig relations[27] require that $f(\omega)$ and $g(\omega)$ are odd and even functions of ω, respectively. Although use of an asymmetrised absorption line shape, for example:
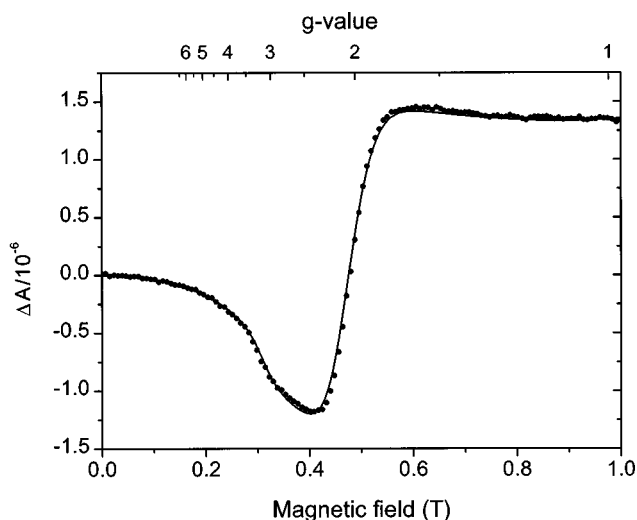

FIG. 2. PROD spectrum of *Pseudomonas aeruginosa* cytochrome c_{551} measured at 588 nm (points). An argon ion pumped ring-dye laser was used as the optical source. The optical power incident on the sample was 17.5 mW. The optical pathlength was 0.5 mm. The sample concentration estimated from the optical absorption spectrum was 2.6 mM. The sample was immersed in super-fluid helium at 1.8 K. The microwave field had a frequency $\omega/2\pi$ of 13.66 GHz and an amplitude $2B_1\cong1$ G. The absorptive phase signal is completely microwave power saturated under these conditions. A dispersive phase simulation with $|C_{zz}|\gg|C_{xx}|,|C_{yy}|$ (line) provides an excellent fit to the data.
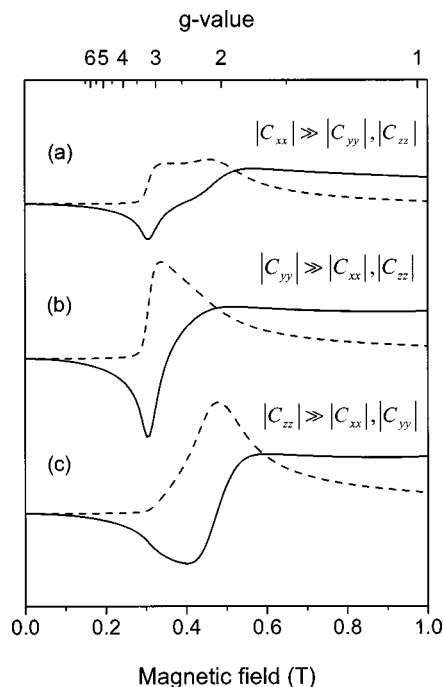
g-value

FIG. 3. Simulated 13.66 GHz PROD line shapes of *Pseudomonas aeruginosa* cytochrome c$_{551}$ using a rhombic spin Hamiltonian ($g_x = 0.8$, $g_y = 2.03$, $g_z = 3.2$) and Eq. (15). The three limiting cases of MCD anisotropy are shown, $|C_{xx}| \gg |C_{yy}|, |C_{zz}|$ (a), $|C_{yy}| \gg |C_{xx}|, |C_{zz}|$ (b), and $|C_{zz}| \gg |C_{xx}|, |C_{yy}|$ (c). A Gaussian distribution of crystal field parameters is used to simulate the dominant ''g-strain'' broadening in this protein (Ref. 31). Both the dispersive (solid lines) and absorptive (dashed lines) phase spectra are shown.

$$f(\omega) = \frac{1}{\pi} \left\{ \frac{\Delta\omega}{(\omega_0 - \omega)^2 + (\Delta\omega)^2} - \frac{\Delta\omega}{(\omega_0 + \omega)^2 + (\Delta\omega)^2} \right\},$$

where $\Delta\omega$ is a linewidth parameter, is usually not necessary, use of a symmetrized dispersion line shape, for example,

$$g(\omega) = \frac{1}{\pi} \left\{ \frac{(\omega_0 - \omega)}{(\omega_0 - \omega)^2 + (\Delta\omega)^2} + \frac{(\omega_0 + \omega)}{(\omega_0 + \omega)^2 + (\Delta\omega)^2} \right\},$$

makes an important adjustment to the dispersion line shapes of broad ''powder'' spectra.

Low spin ferric Haem centres have a rhombic fictitious spin-1/2 spin Hamiltonian. They therefore provide a test of the most general form of the theory presented earlier, Eq. (15). The PROD spectrum of *Pseudomonas aeruginosa* cytochrome c$_{551}$ measured at 588 nm is shown in Fig. 2. According to the theory described above, the spectrum can be any linear combination of the spectral line shapes obtained for the three limiting cases shown in Fig. 3, $|C_{xx}| \gg |C_{yy}|, |C_{zz}|$, $|C_{yy}| \gg |C_{xx}|, |C_{zz}|$, and $|C_{zz}| \gg |C_{xx}|, |C_{yy}|$. It is found, however, that the single limiting case $|C_{zz}| \gg |C_{xx}|, |C_{yy}|$ provides an excellent fit to the data. The optical wavelength dependence of the cytochrome c$_{551}$ PROD signal has been published elsewhere.[20]

IV. CONCLUSION

The expressions required to simulate the PROD line shapes of molecules with fictitious spin-1/2 ground levels has been derived. Using these expressions it has been possible to simulate accurately a biological transition metal ion

center, low spin ferric Haem, with a rhombic spin Hamiltonian, Fig. 2. The same theory has also successfully simulated a number of other metalloprotein systems including the type 1 (''blue'') copper center of *Pseudomonas aeruginosa* azurin,[21] which has an approximately axial spin Hamiltonian. Since these centers exhibit very different optical and magnetic properties, this is strong evidence for the validity of the theoretical model used.

The line shapes are strongly dependent on the anisotropy of the magnetic circular dichroism, Fig. 3. In comparison, the MCD magnetization/saturation experiment shows a relative subtle dependence on this anisotropy.[6] As noted above, this improvement is due to the superior magnetic resolution of the electron paramagnetic resonance experiment. The additional orientational information obtained with the PROD experiment is potentially very useful in the understanding of molecular structure. By studying the optical wavelength dependence of the PROD line shape, the method is able to deconvolute overlapping optical bands with only subtly different MCD anisotropies.

Further improvements in the accuracy with which MCD anisotropy can be measured with the PROD experiment are expected from increasing the microwave frequency. Similar theoretical methods to those described here can be used for systems with $\widetilde{S} > \frac{1}{2}$ ground levels. Work in these directions is underway at present. Instruments covering the 400–1600 nm range under are construction.

APPENDIX A: DERIVATION OF EQUATION (1)

We start from the equation of Schatz *et al.*[3] for the orientational dependence of the MCD observed along the laboratory axis P in the symmetrised form of Oganesyan *et al.*:[5]

$$\Delta\varepsilon_P = -\frac{K}{Q'} \sum_{i,j,k} \varepsilon_{ijk} A_{Pk} \sum_{g,e} \text{Im}\{\langle g'|m_i|e'\rangle$$

$$\times \langle e'|m_j|g'\rangle\} \exp\left(-\frac{E_g'}{kT}\right) f'(\nu, \nu_{eg}, \Delta_{eg}), \quad (A1)$$

where $|g\rangle$ are the ground level eigenstates, ε_{ijk} is the antisymmetric Levi–Civita tensor, E_g is the energy of a ground state, and Q is the partition function. Primed quantities are potentially magnetic field dependent. However, for paramagnetic molecules at cryogenic temperatures, the dominant contribution to the MCD arises from thermal population differences between the ground states. In common with other theories,[3,28] we may therefore approximate Eq. (A1) by taking the line shape function $f(\nu, \nu_{eg}, \Delta_{eg})$ as independent of

J. Chem. Phys., Vol. 113, No. 10, 8 September 2000

Magnetic circular dichroism anisotropy   4337

the applied magnetic field. For an isolated Kramers doublet, the ground level states $|g\rangle$ are also independent of magnetic field. Provided that the magnetic field only mixes the excited level states $|e\rangle$ within themselves, the sum over $|e\rangle$ removes the need to consider the magnetic field, and also the orientational, dependence of these states[28] (the principle of spectroscopic stability):

$$\Delta\varepsilon_P = -\frac{K}{Q'}f(\nu,\Delta)\sum_{i,j,k}\varepsilon_{ijk}A_{Pk}\sum_{g,e}\ \mathrm{Im}\{\langle g|m_i|e\rangle$$

$$\times\langle e|m_j|g\rangle\}\exp\left(-\frac{E_g'}{kT}\right). \tag{A2}$$

The MCD orientational dependence now resides in the directional cosines A_{Pk} the normalized populations $(1/Q')\times\exp(-E_g'/kT)$ and the ground level states, $|g\rangle$ and its Kramers conjugate $|\bar{g}\rangle$.

Essentially, the derivation of Eq. (1) involves the reformulation of Eq. (A2) in terms of the density matrix method of statistical mechanics.[29] We shall focus on the quantity

$$\mathrm{Im}\left\{\overline{\left\langle \sum_e m_i|e\rangle\langle e|m_j\right\rangle}\right\}=\frac{1}{Q'}\sum_{g,e}\ \mathrm{Im}\{\langle g|m_i|e\rangle$$

$$\times\langle e|m_j|g\rangle\}\exp\left(-\frac{E_g'}{kT}\right),$$

which is the thermal ensemble average of the ''MCD operator:'' $\mathrm{Im}\{\Sigma_e m_i|e\rangle\langle e|m_j\}$. The possible states of an individual molecule, $|g\rangle$ may be expressed in terms of a *molecule fixed* basis $|g(z)\rangle$, $|\bar{g}(z)\rangle$ as $|g\rangle=c_1|g(z)\rangle+c_2|\bar{g}(z)\rangle$, where c_i are complex numbers. The density matrix $\boldsymbol{\rho}$ is defined by $\rho_{ij}=\overline{c_j^*c_i}$, the ensemble average of $c_j^*c_i$. It can be expressed as

$$\boldsymbol{\rho}=\tfrac{1}{2}\mathbf{1}+\langle\tilde{S}_x\rangle\boldsymbol{\sigma}_x+\langle\tilde{S}_y\rangle\boldsymbol{\sigma}_y+\langle\tilde{S}_z\rangle\boldsymbol{\sigma}_z,$$

where

$$\boldsymbol{\sigma}_x=\begin{pmatrix}0&1\\1&0\end{pmatrix},\quad \boldsymbol{\sigma}_y=\begin{pmatrix}0&-i\\i&0\end{pmatrix},\quad \boldsymbol{\sigma}_z=\begin{pmatrix}1&0\\0&-1\end{pmatrix},$$

are the Pauli matrices and $\langle\tilde{S}_{x,y,z}\rangle$ are real numbers. In EPR theory[7] the parameters $\langle\tilde{S}_{x,y,z}\rangle$ are *defined* as the three components of the *fictitious* spin. The states $|g(z)\rangle$, $|\bar{g}(z)\rangle$ are then regarded as fictitious spin functions quantised along a molecular axis, which we arbitrarily call z. The ensemble averaged expectation value of $\Sigma_e m_i|e\rangle\langle e|m_j$ is given by

$$\overline{\left\langle\sum_e m_i|e\rangle\langle e|m_j\right\rangle}=\mathrm{tr}\left\{\boldsymbol{\rho}\left[\sum_e m_i|e\rangle\langle e|m_j\right]\right\}. \tag{A3}$$

We need to know the form of the matrix $[\Sigma_e m_i|e\rangle\langle e|m_j]$ in the basis $|g(z)\rangle$, $|\bar{g}(z)\rangle$. Noting that m_{ijk} are time even operators one finds that

$$\sum_e \langle g(z)|m_i|e\rangle\langle e|m_j|g(z)\rangle$$

$$=\left(\sum_e \langle\bar{g}(z)|m_i|e\rangle\langle e|m_j|\bar{g}(z)\rangle\right)^*$$

and

$$\sum_e \langle g(z)|m_i|e\rangle\langle e|m_j|\bar{g}(z)\rangle$$

$$=-\left(\sum_e \langle\bar{g}(z)|m_i|e\rangle\langle e|m_j|g(z)\rangle\right)^*.$$

The matrix $[\Sigma_e m_i|e\rangle\langle e|m_j]$ must therefore take the form

$$\left[\sum_e m_i|e\rangle\langle e|m_j\right]=\begin{pmatrix}p&q\\-q^*&p^*\end{pmatrix},$$

where $p=\Sigma_e\langle g(z)|m_i|e\rangle\langle e|m_j|g(z)\rangle$ and $q=\Sigma_e\langle g(z)|m_i|e\rangle\langle e|m_j|\bar{g}(z)\rangle$. Inserting into Eq. (A3) one finds:

$$\mathrm{Im}\left\{\overline{\left\langle\sum_e m_i|e\rangle\langle e|m_j\right\rangle}\right\}=2[\mathrm{Im}\{q\}\langle\tilde{S}_x\rangle+\mathrm{Re}\{q\}\langle\tilde{S}_y\rangle$$

$$+\mathrm{Im}\{p\}\langle\tilde{S}_z\rangle].$$

The expression may be made more symmetrical by introducing additional basis functions: $|g(x)\rangle=(1/\sqrt{2})(|g(z)\rangle+|\bar{g}(z)\rangle)$, $|\bar{g}(x)\rangle=(1/\sqrt{2})(|g(z)\rangle-|\bar{g}(z)\rangle)$, $|g(y)\rangle=(1/\sqrt{2})(|\bar{g}(z)\rangle-|g(z)\rangle)$, $|\bar{g}(y)\rangle=(1/\sqrt{2})(|g(z)\rangle-i|\bar{g}(z)\rangle)$, defined in such a way that the unitary transformations between the bases $(|g(z)\rangle,|\bar{g}(z)\rangle)$, $(|g(x)\rangle,|\bar{g}(x)\rangle)$, and $(|g(y)\rangle,|\bar{g}(y)\rangle)$ are equivalent to the analogous rotations of true spin-1/2 functions.[30] The bases $(|g(x)\rangle,|\bar{g}(x)\rangle)$, and $(|g(y)\rangle,|\bar{g}(y)\rangle)$ are (within an arbitrary phase factor) therefore the fictitious spin functions quantized along the molecular x and y axes, respectively. Expressing q in terms of $|g(x)\rangle$, $|\bar{g}(x)\rangle$, and $|g(y)\rangle$, $|\bar{g}(y)\rangle$ one finds

$$\mathrm{Im}\left\{\overline{\left\langle\sum_e m_i|e\rangle\langle e|m_j\right\rangle}\right\}$$

$$=2\left[\mathrm{Im}\left\{\sum_e\langle g(x)|m_i|e\rangle\langle e|m_j|g(x)\rangle\right\}\langle\tilde{S}_x\rangle\right.$$

$$+\mathrm{Im}\left\{\sum_e\langle g(y)|m_i|e\rangle\langle e|m_j|g(y)\rangle\right\}\langle\tilde{S}_y\rangle$$

$$\left.+\mathrm{Im}\left\{\sum_e\langle g(z)|m_i|e\rangle\langle e|m_j|g(z)\rangle\right\}\langle\tilde{S}_z\rangle\right].$$

Inserting this expression into Eq. (A2) for each i, j, and noting that

$$\mathrm{Im}\left\{\overline{\left\langle\sum_e m_i|e\rangle\langle e|m_j\right\rangle}\right\}=-\mathrm{Im}\left\{\overline{\left\langle\sum_e m_j|e\rangle\langle e|m_i\right\rangle}\right\}$$

one obtains Eq. (1).

APPENDIX B: DIAGONALISATION OF THE ZEEMAN HAMILTONIAN

Although diagonalization of a fictitious spin-1/2 spin Hamiltonian has been previously described in the literature,[3,4,6] we shall provide an explicit derivation because we require the orientation of the axis z_Q along which the fictitious spin is quantized. We consider a molecule with a rhombic g-value system $(g_x\neq g_y\neq g_z)$. Let the applied magnetic field be orientated with respect to the g-value axis sys-
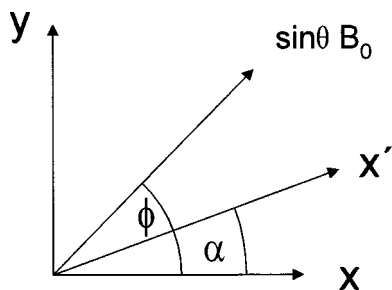
FIG. 4. Definition of x' axis and angle α.

tem in accordance with Fig. 1. We consider first the component of B_0 lying in the g-value xy plane, Fig. 4. Once allowance is made for the g-value anisotropy, the effective field in the xy plane lies along x'. The angle α is related to ϕ by $\sin\alpha = (g_y/g_\perp)\sin\phi$, $\cos\alpha = (g_x/g_\perp)\cos\phi$, where $g_\perp^2 = g_y^2\sin^2\phi + g_x^2\cos^2\phi$. z_Q must lie in the plane containing the g-value z axis and x', Fig. 5. Angle β is related to θ by an analogous set of equations: $\sin\beta = (g_\perp/g)\sin\theta$, $\cos\beta = (g_z/g)\cos\theta$, $g^2 = g_\perp^2\sin^2\theta + g_z^2\cos^2\theta$. This completes the determination of z_Q, and hence the diagonalization of the Zeeman Hamiltonian. The component of $\langle\tilde{S}_0\rangle$ along the ith principal g-value axis is $\langle\tilde{S}_i\rangle = A_{z_Qi}\langle\tilde{S}_0\rangle$, Fig. 5. By expressing the A_{z_Qi} in terms of θ and ϕ using the expressions given above one obtains Eq. (2).

APPENDIX C: SOLUTION OF THE EQUATION OF MOTION OF $\langle\tilde{S}\rangle$

Excitation with a microwave field will cause $\langle\tilde{S}\rangle$ to precess in a plane perpendicular to the fictitious spin quantization axis z_Q calculated in Appendix B. The axes x'' and y' lie in this plane, Fig. 5. The microwave field is applied along the laboratory X axis. The component along the ith g-value axis is $B_{1i} = A_{Xi}B_1$, Fig. 1. The component of the transition dipole along x'' is therefore

$$g_{x''} = \left(\frac{g_\perp g_z}{g}\right)\cos\eta + \left(\frac{(g_y^2 - g_x^2)g_z}{g_\perp g}\right)\cos\phi\sin\phi\cos\theta\sin\eta.$$
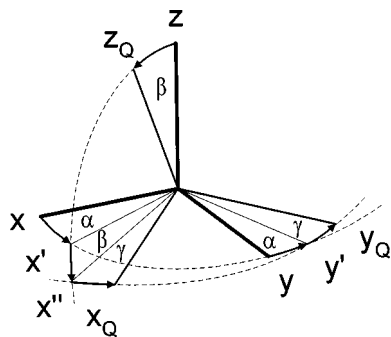(C1)

The component along y' is

FIG. 5. Euler angles α, β, γ relating the ''quantization'' axis system x_Q, y_Q, z_Q to the molecular g-value axis system x, y, z. Explicit expressions for the directional cosines A_{x_Q}, A_{y_Q}, and A_{z_Q} used in the main text are obtained from those for A_X, A_Y, and A_Z (Fig. 1) by pairwise substitution of (α,β,γ) for (ϕ,θ,η).

$$g_{y'} = \left(\frac{g_x g_y}{g_\perp}\right)\sin\eta.$$
(C2)

We now introduce our final axes $x_Q y_Q$ rotated relative to $x''y'$ by an angle γ (Fig. 5):

$$\sin\gamma = \frac{g_{y'}}{g_1}, \quad \cos\gamma = \frac{g_{x''}}{g_1},$$

where

$$g_1^2 = g_{x''}^2 + g_{y'}^2.$$
(C3)

The significance of the axis x_Q is that it is the direction along which the effective microwave field lies. Our expression for g_1, the combined transition matrix element, Eq. (12), is obtained by substituting Eqs. (C1) and (C2) into Eq. (C3). Once an average over η is performed, Eq. (12) is equivalent to the expressions previously derived in the context of conventional EPR spectroscopy.[7,8]

Importantly, we have explicitly derived an axis system $x_Q y_Q z_Q$ in which the motion of the fictitious spin is particularly simple. The system will behave like an isotropic system with a field applied along z_Q and a linearly polarized microwave field applied along x_Q. We may calculate the motion of the fictitious spin in the frame $x_Q y_Q z_Q$ with any of the well known approaches of magnetic resonance.[25] Generally, we can write $\langle\tilde{S}_{x_Q}\rangle = \langle\tilde{S}_{\text{disp.}}\rangle\cos(\omega t) - \langle\tilde{S}_{\text{abs.}}\rangle\sin(\omega t)$, $\langle\tilde{S}_{y_Q}\rangle = \langle\tilde{S}_{\text{disp.}}\rangle\sin(\omega t) + \langle\tilde{S}_{\text{abs.}}\rangle\cos(\omega t)$, where $\langle\tilde{S}_{\text{abs.}}\rangle$ and $\langle\tilde{S}_{\text{disp.}}\rangle$ are the oscillating fictitious spin components responsible for the conventional EPR absorption and dispersion, respectively.

We now wish to know the projections of these oscillating fictitious spin polarizations onto the g-value axes. Our notation reflects the fact that only $\langle\tilde{S}_{x_Q}\rangle$ will generate a conventional EPR signal in an instrument employing linearly polarized microwaves: $\langle\tilde{S}_{y_Q}\rangle$ does not generate an oscillating magnetic dipole along X. Inspection of Fig. 5 gives for the ith g-value axis: $\langle\tilde{S}_i\rangle_{\text{EPR}} = A_{x_Qi}\langle\tilde{S}_{x_Q}\rangle$ and $\langle\tilde{S}_i\rangle_{\text{Quad.}} = A_{y_Qi}\langle\tilde{S}_{y_Q}\rangle$. By expressing the directional cosines in terms of θ, ϕ, and η using previous expressions one obtains Eqs. (6)–(11).

[1] A. J. Thomson, M. R. Cheesman, and S. J. George, Methods Enzymol. **226**, 199 (1993).

[2] J. A. Farrar, F. Neese, P. Lappalainen, P. M. H. Kroneck, M. Sarraste, W. G. Zumft, and A. J. Thomson, J. Am. Chem. Soc. **118**, 11501 (1996).

[3] P. N. Schatz, R. L. Mowery, and E. R. Krausz, Mol. Phys. **35**, 1537 (1978).

[4] A. J. Thomson and M. K. Johnson, Biochem. J. **191**, 411 (1980).

[5] V. S. Oganesyan, S. J. George, M. R. Cheesman, and A. J. Thomson, J. Chem. Phys. **110**, 762 (1999).

[6] F. Neese and E. I. Solomon, Inorg. Chem. **38**, 1847 (1999).

[7] A. Abragam and B. Bleaney, *Electron Paramagnetic Resonance of Transition Ions* (Oxford University Press, Oxford, 1970).

[8] J. R. Pilbrow, *Transition Ion Electron Paramagnetic Resonance* (Oxford University Press, Oxford, 1990).

[9] C. P. Barrett, J. Peterson, C. Greenwood, and A. J. Thomson, J. Am. Chem. Soc. **108**, 3170 (1986).

[10] A. J. Thomson, C. Greenwood, J. Peterson, and C. P. Barrett, J. Inorg. Biochem. **28**, 195 (1986).

[11] A. Kastler, C. R. Paris Acad. Sci. **232**, 953 (1951).

[12] S. Geschwind, in *Electron Paramagnetic Resonance*, edited by S. Geschwind (Plenum, New York, 1972).

[13] N. Bloembergen, S. Shapiro, P. S. Pershan, and J. O. Artman, Phys. Rev. **114**, 445 (1959).

[14] Y. R. Shen, *The Principles of Nonlinear Optics*, 1st ed. (Wiley, New York, 1984).

[15] D. Suter, *The Physics of Laser Atom Interactions* (Cambridge University Press, Cambridge, 1997).

[16] N. C. Wong, E. S. Kintzer, J. Mlynek, R. G. DeVoe, and R. G. Brewer, Phys. Rev. B **28**, 4993 (1983).

[17] H. G. Dehmelt, Phys. Rev. **105**, 1924 (1957).

[18] N. Bloembergen, P. S. Pershan, and L. R. Wilcox, Phys. Rev. **120**, 2014 (1960).

[19] S. J. Bingham, D. Suter, A. Schweiger, and A. J. Thomson, Chem. Phys. Lett. **266**, 543 (1997).

[20] B. Börger, S. J. Bingham, J. Gutschank, M.-O. Schweika, D. Suter, and A. J. Thomson, J. Chem. Phys. **111**, 8565 (1999).

[21] S. J. Bingham, B. Börger, J. Gutschank, D. Suter, and A. J. Thomson, J. Biol. Inorg. Chem. **5**, 30 (2000).

[22] K. Holliday, X. F. He, P. T. H. Fisk, and N. B. Manson, Opt. Lett. **15**, 983 (1990).

[23] S. J. Bingham, B. Börger, D. Suter, and A. J. Thomson, Rev. Sci. Instrum. **69**, 3403 (1998).

[24] T. H. Wilmshurst, *Electron Spin Resonance Spectrometers* (Adam Hilger, London, 1967).

[25] A. Abragam, *The Principles of Nuclear Magnetism* (Oxford University Press, Oxford, 1961).

[26] J. J. R. Frausto da Silva and R. J. P. Williams, *The Biological Chemistry of the Elements* (Oxford University Press, Oxford, 1991).

[27] C. P. Slichter, *Principles of Magnetic Resonance*, 1st ed. (Harper, New York, 1963).

[28] P. J. Stephens, Adv. Chem. Phys. **35**, 197 (1976).

[29] R. C. Tolman, *The Principles of Statistical Mechanics* (Oxford University Press, Oxford, 1938).

[30] D. M. Brink and G. R. Satchler, *Angular Momentum*, 2nd ed. (Oxford University Press, Oxford, 1968).

[31] W. R. Hagen, J. Magn. Reson. **44**, 447 (1981).